PHOTOCONVERSION OF CO_2 USING COPPER-MODIFIED TITANIUM DIOXIDE NANOPARTICLES

Jing WEI[1], Xin TAN[2], Tao YU[3,*] and Lin ZHAO[4]

School of Environmental Science and Engineering, Tianjin University, Tianjin 300072, China; e-mail: [1] weijing@tju.edu.cn, [2] tanxin@tju.edu.cn, [3] lisat.yu@gmail.com, [4] zhaolin@tju.edu.cn

Received March 5, 2011
Accepted May 25, 2011
Published onine November 20, 2011

A series of copper-modified titanium dioxide (Cu/TiO_2) nanoparticles were synthesized via one-step sol-gel method. The crystal structure and chemical properties were characterized using X-ray diffraction (XRD) and X-ray photoelectron spectroscopy (XPS). The Cu/TiO_2 nanoparticles were applied to CO_2 photoconversion and the yield of formaldehyde was used to evaluate the photocatalytic performance. The optimum amount of copper modifying was 0.6 wt.% and the yield of formaldehyde was 946 $\mu mol/g_{cat}$ under UV illumination for 6 h. 20 wt.% Cu/TiO_2 also performed a high photocatalytic activity, which yielded 433 $\mu mol/g_{cat}$ formaldehyde under UV illumination for 6 h.

Keywords: Photoconversion; Carbon dioxide; Formaldehyde; Titanium dioxide; Copper; Environmental chemistry; Photolysis; Materials science.

Nowadays, the increasing emission of carbon dioxide has accelerated the greenhouse effect. In response, the Kyoto Protocol of the United Nations Framework Convention on Climate Change mandated a return of CO_2 emission levels to those of 1990 [1]. The conversion of CO_2 into formaldehyde, formic acid, methane, methanol and other hydrocarbons is essential in developing alternative fuels and various raw materials for different chemical industries[2–6].

Titanium dioxide, with the low band-gap values of about 3.2 eV for anatase phase, can fulfill the thermodynamic requirements of most photocatalytic reactions and it is also valued for its chemical stability, lack of toxicity and low cost[7–9]. Doping impurities can inhibit the recombination of photogenerated e^-/h^+ pairs, so as to enhance the photocatalytic activity of TiO_2 [10–12].

A number of researchers have demonstrated that copper-modified TiO_2 nanoparticles (NPs) are favorable to CO_2 conversion[13–15]. Adachi et al.[16] reported that under the condition of the Cu/TiO_2 NPs illuminated with a Xe

doi:10.1135/cccc2011057

lamp, and also pressurized with CO_2 of 2.8 MPa, the products were specific for methane, ethylene and ethane. Tseng et al.[1] reported that the methanol yield of 2.0 wt.% Cu/TiO_2 was 118 μmol/g under UV illumination for 6 h, while only 4.7 μmol/g methanol yielded over bare TiO_2 NPs under the same condition. Yamashita et al.[17] reported that incorporation of copper(II) into the TiO_2 matrix can improve the selectivity of methanol and also can increase the efficiency of CO_2 conversion. Although many investigators noted that the addition of copper could improve the photocatalytic activity in CO_2 reduction, it is still not clear which copper species (Cu^0, Cu^{1+}, or Cu^{2+}) is responsible for this phenomenon.

In this study, the photocatalytic activity was evaluated using the products measurement of CO_2 photoconversion under UV light irradiation. A series of copper-modified TiO_2 NPs was synthesized via sol-gel method and was characterized by X-ray diffraction and X-ray photoelectron spectroscopy. The different effects of copper species were studied with respect to the characteristics of Cu/TiO_2 NPs, and the possible mechanisms were further discussed in detail.

EXPERIMENTAL

Photocatalyst Preparation

Bare TiO_2 (denoted as BT) and copper-modified TiO_2 (denoted as Cu/TiO_2) were synthesized using a one-step sol-gel technique. First, 5 ml $Ti(O\text{-}Bu)_4$ was dissolved in 30 ml absolute ethanol and stirred in beaker A for 30 min to get a homogeneous solution. Various amount of cupric nitrate (the mass ratio of copper and titanium were 0.001, 0.006, 0.02, 0.07, 0.2 and 0.3, respectively) were dissolved in a mixture of 20 ml absolute ethanol, 1.5 ml double distilled water and 0.7 ml nitric acid in beaker B. Under the magnetically stirring, the solution in beaker B was added slowly into beaker A. The resulting transparent blue sol was dried at 82 °C for 2 h and calcined in flowing air at 500 °C for 2 h. The NPs were then ground.

Characterization

X-ray diffraction (XRD) analysis was carried out on an X-ray diffractometer (Rigaku D/max 2500, Japan) in the 2θ range between 10–90° using CuKα (λ = 0.15418 nm) as radiation source, the accelerating voltage of 40 kV and a current of 200 mA with a scan speed of 0.02°/min were employed to analyze the phase state and crystal structure of the synthesized NPs. The crystallite size was calculated using Scherrer equation[18]

$$\Phi = K\,\lambda/\beta\,\cos\theta \qquad (1)$$

where Φ is the crystallite size, K is the shape factor, λ is the wave length, β is the full width at half maximum of peak of 101 planes of anatase and θ is the diffracting angle. X-ray photoelectron spectroscopy (XPS) conducted using a PHI-1600 ESCA system was employed to characterize the chemical state of modified copper in the compounds as well as the other

chemical ingredients of the synthesized samples. In the XPS process, an MgKα X-ray beam was used in a vacuum chamber at 2×10^{-10} torr. The depth of analysis was 20–50 Å.

Photocatalytic Reaction

The photoconversion of CO_2 was carried out in a SGY-I photochemical reactor, equipped with N_2 bubbling, a quartz cool trap, and 50 ml quartz reactors. Aqueous slurries were prepared by adding 1 g/l NPs into 0.2 mol/l NaOH aqueous solution. The system was illuminated by a 300 W Hg lamp with a main peak light intensity at 365 nm in the side of the reactor. The aqueous slurries were bubbled with the mixture of N_2 and 30 ml/min CO_2 (the purity was 99.999%) during the reaction. Prior to the illumination, the aqueous slurries were bubbled for 0.5 h to ensure that all dissolved oxygen was eliminated. Blank reactions were conducted to ensure that the yield of formaldehyde was due to the photoconversion of CO_2, and also to eliminate the surrounding interferences. One blank experiment was UV-illuminated without the NPs, and the other was in the dark with the NPs and CO_2 under the same experimental conditions. An additional blank test was the NPs filling N_2 without CO_2. No formaldehyde was detected in the above three blank tests. The yield of formaldehyde was analyzed using gas chromatograph (Agilent 6890N), which equipped with a DB-624 capillary column (30 m × 0.53 mm × 3 μm).

RESULTS AND DISCUSSION

Catalyst Characterizations

X-ray diffraction patterns of different NPs are shown in Fig. 1 and XRD determined average crystal sizes are shown in Table I.

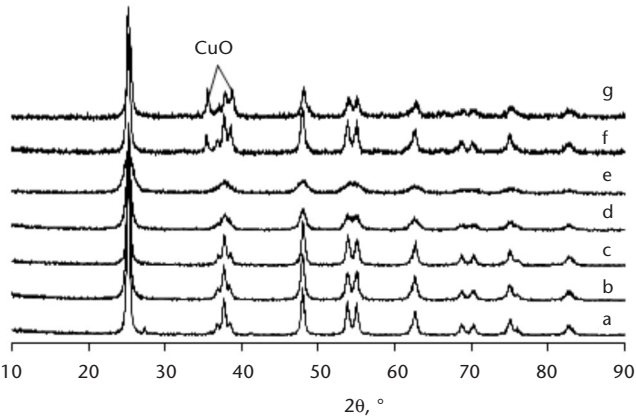

FIG. 1
X-ray diffraction patterns of different NPs: TiO_2 (a), 0.1 wt.% Cu/TiO_2 (b), 0.6 wt.% Cu/TiO_2 (c), 2 wt.% Cu/TiO_2 (d), 7 wt.% Cu/TiO_2 (e), 20 wt.% Cu/TiO_2 (f), 30 wt.% Cu/TiO_2 (g)

Figure 1 shows that in the series of copper modifying ratio less than 7 wt.%, the characteristic peaks of Cu/TiO_2 broadened with the increasing of copper amount. We also can see that two characteristic peaks at 35.54 and 38.76° according to cubic CuO (JCPDS 65-2309 and JCPDS 44-0706) were observed when the copper modifying ratio was above 20 wt.%. The intensity increased with the increasing concentration of copper modifying ratio. No other phases, such as Cu_2O or Cu, were found in XRD patterns. As shown in Table I, the grain sizes of *x* wt.% Cu/TiO_2 NPs were all smaller than bare TiO_2 NPs, which was consistent with the results calculated by Scherrer's formula. It has been thought that the copper modifying reduced the crystallization of anatase and retarded the transformation of amorphous TiO_2 to anatase[12].

TEM images of different NPs are shown in Fig. 2. It can be seen from Fig. 2 that the nanocrystal size of BT and *x* wt.% Cu/TiO_2 were all smaller than 20 nm. The results were in general agreement with the XRD determination. When the copper modifying ratio was less than 7 wt.%, with the addition of copper increased, the crystal size of nanoparticles gradually decreased, which reveals the modifying of copper retarded the crystallization of TiO_2. When the copper modifying ratio was more than 20 wt.%, the crystal size of nanoparticles was bigger than BT, which because of the synthesized materials was not just TiO_2, but the compound semiconductor of TiO_2 and CuO. It can also be seen from Fig. 2 that the synthesized nanoparticles were not well dispersed. However, we can still clearly see the shape of grains and the lattice fringes, which mean the crystallization of synthesized nanoparticles, were in good condition.

TABLE I
Average crystal size of *x* wt.% Cu/TiO_2 NPs

Synthesized NPs	Crystal size[a] (nm)
TiO_2	18.9
0.1 wt.% Cu/TiO_2	16.4
0.6 wt.% Cu/TiO_2	15.2
2 wt.% Cu/TiO_2	12.9
7 wt.% Cu/TiO_2	11.7
20 wt.% Cu/TiO_2	17.2
30 wt.% Cu/TiO_2	15.1

[a] Calculated from anatase 101 crystal face.

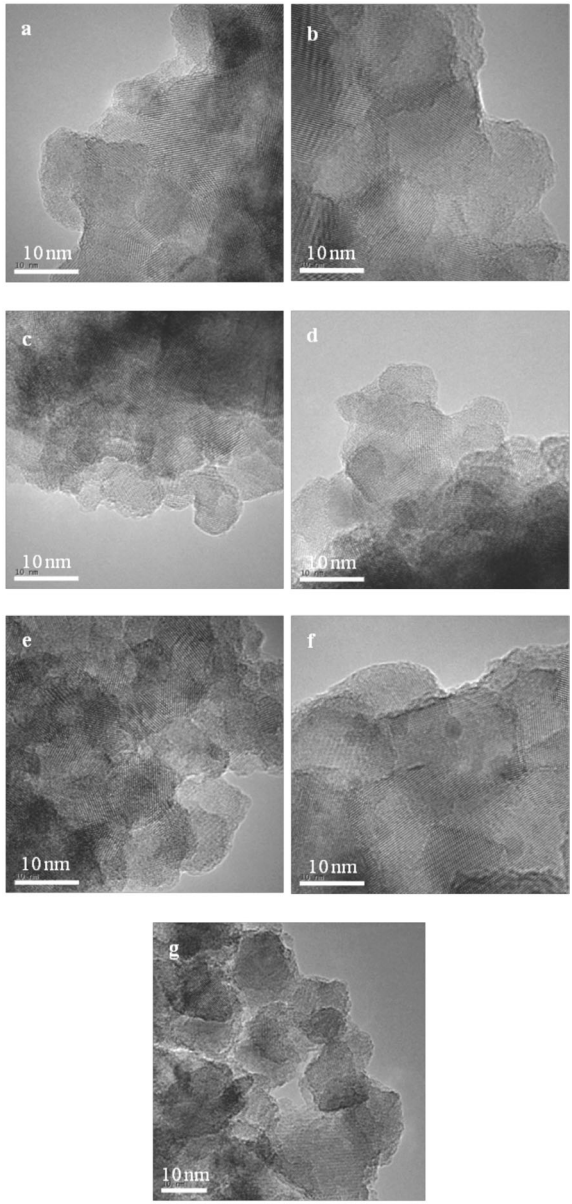

FIG. 2
TEM images of *x* wt.% Cu/TiO_2: BT (a), 0.1 wt.% Cu/TiO_2 (b), 0.6 wt.% Cu/TiO_2 (c), 2 wt.% Cu/TiO_2 (d), 7 wt.% Cu/TiO_2 (e), 20 wt.% Cu/TiO_2 (f), 30 wt.% Cu/TiO_2 (g)

In Fig. 3, the Ti 2p XPS of synthesized *x* wt.% Cu/TiO_2 ranged from 458.3 to 458.5 eV, and BT's Ti 2p binding energy was 458.4 eV. It was indicated that the titanium element mainly existed as Ti^{4+}, and the loading of copper did not induce its chemical shift. The O 1s XPS spectra show a prominent peak at around 530 eV, which was ascribed to the lattice oxygen (O_{lat}) in TiO_2. The O 1s XPS deconvoluted spectra of 20 and 30 wt.% Cu/TiO_2 are shown in Fig. 4. From the deconvoluted spectrum, a peak at around 531.9 eV was detected. The oxygen species around this binding energy were observed in adsorbed oxygen containing species (O_{ads}), which were

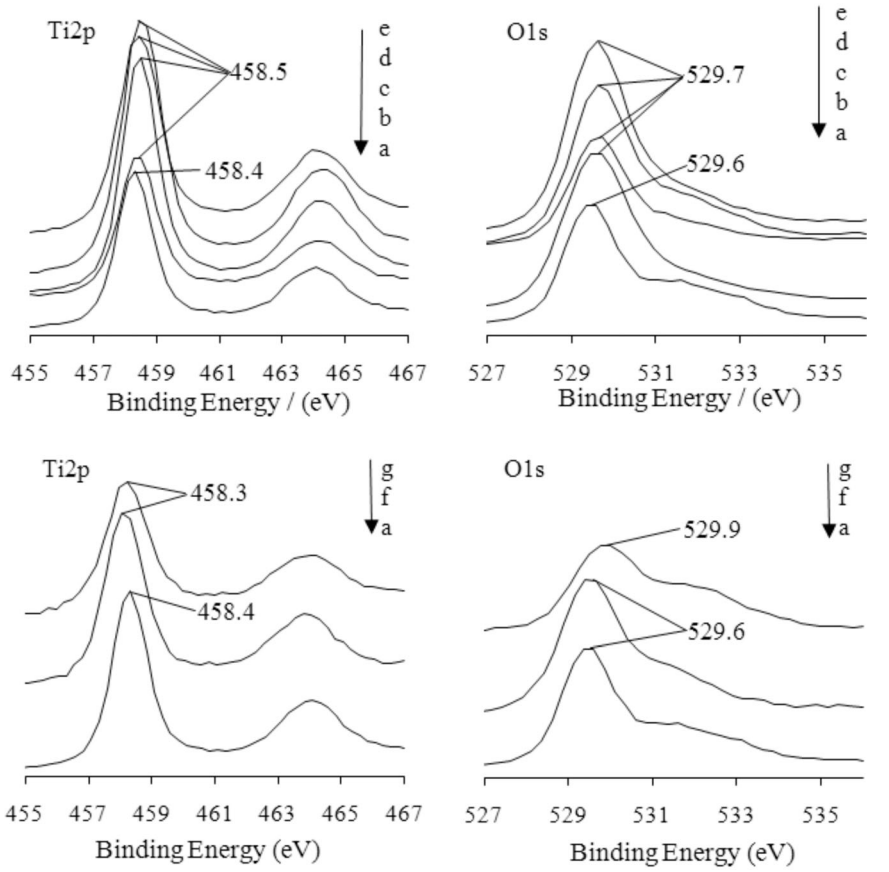

FIG. 3
Ti 2p and O 1s XPS spectra of *x* wt.% Cu/TiO_2: BT (a), 0.1 wt.% Cu/TiO_2 (b), 0.6 wt.% Cu/TiO_2 (c), 2 wt.% Cu/TiO_2 (d), 7 wt.% Cu/TiO_2 (e), 20 wt.% Cu/TiO_2 (f), 30 wt.% Cu/TiO_2 (g)

adsorptive O_2 and/or weekly bonded oxygen species (e.g. hydroxy group)[19]. The percentage of different oxygen species on 20 and 30 wt.% Cu/TiO_2 surfaces was calculated based on their XPS intensities and sensitivities (Fig. 4). O_{ads} content on 30 wt.% Cu/TiO_2 was much higher than that of 20 wt.% Cu/TiO_2. The O_{ads} was an active oxygen species, but played a negative influence in the reduction process.

The Cu 2p XPS spectra of 20 wt.% Cu/TiO_2 and 30 wt.% Cu/TiO_2 are shown in Fig. 5. The binding energy of the Cu 2p peak at around 933.8 eV was indicative of Cu^{2+} species[20], while lower binding energy of 932.4eV was

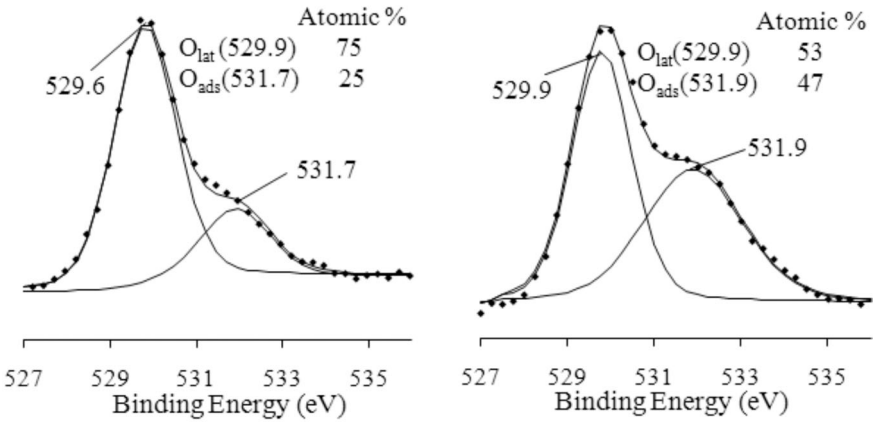

FIG. 4
O 1s XPS deconvoluted spectra of 20 (a) and 30 wt.% Cu/TiO_2 (b)

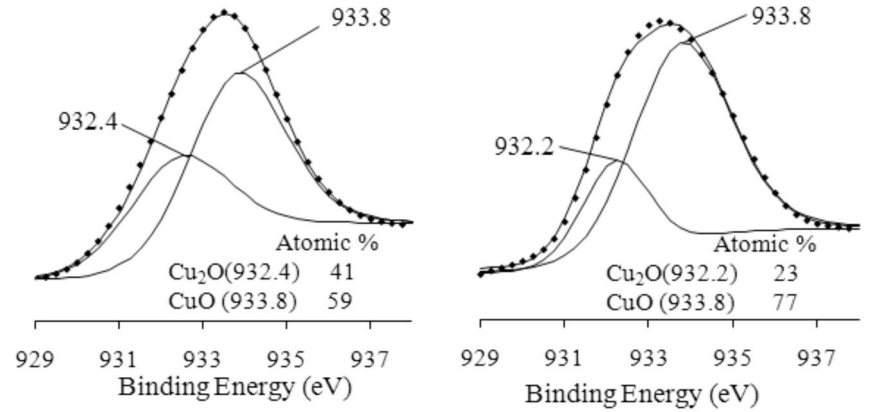

FIG. 5
Cu 2p XPS spectra of 20 (a) and 30 wt.% Cu/TiO_2 (b)

characteristic of Cu^{1+} [21]. The copper species on the surface of both 20 and 30 wt.% Cu/TiO_2 were present as Cu^{2+} and Cu^{1+}. The atomic percentage of Cu^{1+} on the surface of 20 wt.% Cu/TiO_2 was 41% and only 23% on the surface of 30 wt.% Cu/TiO_2. So the 20 wt.% Cu/TiO_2 had a higher atomic percentage of Cu^{1+} on the surface.

Photocatalytic Activities and Mechanism Analysis

Figure 6 shows that the yield of formaldehyde first increased while then decreased with increasing of catalyst concentration. A higher concentration of catalyst was expected to absorb more UV energy, and thus higher formaldehyde yield would be observed. However, the yield of formaldehyde began to decline when the concentration of catalyst exceeded 1 g/l. The penetration of UV light was prevented in the reactor by the large quantity of catalyst in aqueous solution. The UV absorption of the outer catalyst was thus reduced, but the re-oxidation rate of formaldehyde increased with the increasing of catalyst concentration in the reactor[1]. Consequently, the overall formaldehyde yield decreased with excess catalyst.

Figure 7 shows that the yield of formaldehyde first increased and then basically unchanged when the CO_2 flow exceeded 30 ml/min. The bubbling of N_2 could take part of CO_2 away during the reaction. Therefore, one of the methods to maintain the concentration of CO_2 in the reactor and im-

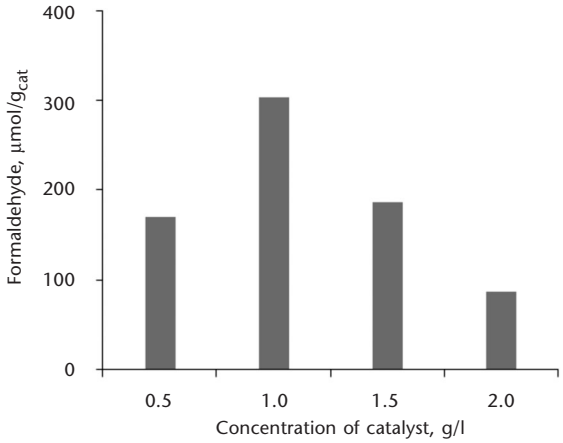

FIG. 6
Effect of catalyst concentration (0.6 wt.% Cu/TiO_2) on formaldehyde yield (reaction time was 6 h)

prove the selective reduction of CO_2 was increasing the flow of CO_2 [22]. When the concentration of CO_2 in the reactor was exceeded the equilibrium concentration, increased yield of formaldehyde could not be obtained with the increasing of CO_2 flow. Figure 7 indicated that when the flow of CO_2 was increased to 30 ml/min or more, the CO_2 flow would not be a rate-limiting step to the reaction.

The photocatalytic activities of Cu/TiO_2 NPs on CO_2 conversion under UV illumination are shown in Fig. 8. When the modified ratio of copper was lower than 7 wt.%, 0.6 wt.% possessed the highest yield of formaldehyde and reached 946 μmol/g_{cat} under UV illumination for 6 h. In the presence of copper clusters, electrons were enriched owing to the alignment of Fermi levels of the metal[23]. Copper served as an electron trapper and avoided the recombination of e^-/h^+ pairs effectively. In addition, the transfer of excited electrons to the copper cluster enhanced the separation of e^-/h^+ pairs, which significantly promoted the photoefficiency[1,24]. Obviously, more copper modification can increase formaldehyde yield because of the increasing amount of trapping sites. While modifying too much, the copper could mask the TiO_2 surface, reducing the photoexciting capacity of TiO_2, and becoming the recombination center. So there was an optimal copper modifying ratio around 0.6 wt.% under the experimental conditions of this work.

By observing the yield of formaldehyde in Fig. 8, the 20 wt.% Cu/TiO_2 also performed a high photocatalytic activity. Figure 1 shows that 20 wt.%

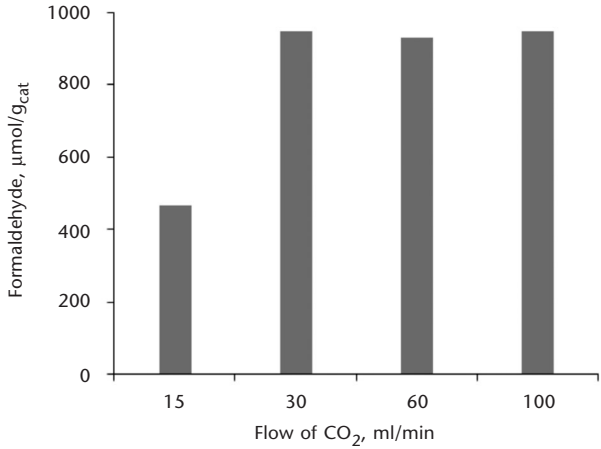

FIG. 7
Effect of CO_2 flow on formaldehyde yield (reaction time was 6 h)

Cu/TiO_2 comprised two phases of TiO_2 and CuO. The conduction band of CuO was more positive than TiO_2, and the generated electrons from CuO were then immigrated to the conduction band of TiO_2. The lifetime of the photogenerated electrons and holes was prolonged during the transfer process, inducing higher quantum efficiency. Since the conduction band edge of CuO was more positive than TiO_2, when the mass ratio of Cu/Ti was increased more than 20 wt.%, CuO could catch electrons from TiO_2 conduction band edge. Consequently, the dopant-trapped electrons were more difficult to be transferred to the adsorbed species on catalyst surface and hence it could be the recombination center of electron/hole pairs[15]. It could be part of the reason that 30 wt.% Cu/TiO_2 had a lower efficiency than 20 wt.% Cu/TiO_2 on the photocatalytic conversion of CO_2. From the analysis of Figs 4 and 5, we can also see that the ratio of the surface elements species on 20 and 30 wt.% Cu/TiO_2 were different. O_{ads} contents on 30 wt.% Cu/TiO_2 were much higher than 20 wt.% Cu/TiO_2. The O_{ads} was an active oxygen species and it can generate $^{\bullet}OH$ radicals which played an important role during the oxidation process[19]

$$O_{ads} + e^- \rightarrow {}^{\bullet}O_2^- \qquad (2)$$

$$^{\bullet}O_2^- + 2\ H^+ \rightarrow 2\ {}^{\bullet}OH \qquad (3)$$

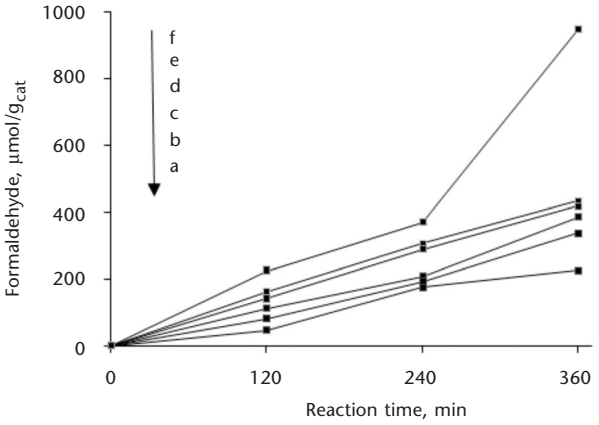

FIG. 8
Photoconversion of CO_2 under UV illumination: 0.1 wt.% Cu/TiO_2 (a), 7 wt.% Cu/TiO_2 (b), 2 wt.% Cu/TiO_2 (c), 30 wt.% Cu/TiO_2 (d), 20 wt.% Cu/TiO_2 (e), 0.6 wt.% Cu/TiO_2 (f)

As to reduction process, too much ·OH was useless. So the different O_{ads} contents could be another part of reason to explain the reason that 30 wt.% Cu/TiO_2 exhibited a lower efficiency than 20 wt.% Cu/TiO_2.

Figure 5 shows that 20 wt.% Cu/TiO_2 had more Cu^{1+} on the surface than 30 wt.% Cu/TiO_2. The redox potential value could represent the ability to attack electrons. The redox potential values for Cu^{1+} and Cu^{2+} were

$$Cu^{2+} + 2e^- \rightarrow Cu^0, \qquad E^0 = 0.34 \text{ eV} \tag{4}$$

$$Cu^{2+} + e^- \rightarrow Cu^{1+}, \qquad E^0 = 0.17 \text{ eV} \tag{5}$$

$$Cu^{1+} + e^- \rightarrow Cu^0, \qquad E^0 = 0.52 \text{ eV}. \tag{6}$$

Cu^{1+} had the highest positive redox potential value and it was more effective to inhibit e^-/h^+ recombination. Wu et al.[25] reported that the existence of Cu^{1+} on the surface of prepared NPs was favorable to the photoreduction process as follows[26]:

$$Cu^{2+} + e^- \rightarrow Cu^{1+} \tag{7}$$

$$Cu^{1+} + C \rightarrow Cu^{2+} + C^*. \tag{8}$$

Cu^{2+} reacted with e^- to form Cu^{1+} and inhibited the combination of e^-/h^+ pairs. In Eq. (*8*), C refers to carbon species, C* refers to the reduced carbon species. Cu^{1+} passed the e^- to carbon species which absorbed on the surface of the NPs, thus accelerated the interfacial electron transfer and promoted the photoreduction process.

CONCLUSIONS

A series of Cu/TiO_2 NPs were synthesized via sol-gel method in this paper. The optimal concentration of catalyst was 1 g/l and the CO_2 flow changes would not be a rate-limiting step in the reaction when the flow of CO_2 was increased to 30 ml/min or more. The 0.6 and 20 wt.% Cu/TiO_2 NPs possessed the higher photoconversion efficiency of CO_2 to formaldehyde under UV irradiation for 6 h. The photocatalytic efficiency of 0.6 wt.% Cu/TiO_2 markedly increased because of lowering the recombination probability for e^-/h^+ pairs, while 20 wt.% Cu/TiO_2 was affected by the contents of CuO, O_{ads} and Cu^{1+} on the surface of NPs.

This work has been supported by the National Natural Science Foundation of China (20776103).

REFERENCES

1. Tseng I., Chang W., Wu J. C. S.: *Appl. Catal., B* **2002**, *37*, 37.
2. Colón G., Maicu M., Hidalgo M. C., Navío J. A.: *Appl. Catal., B* **2006**, *67*, 41.
3. Nguyen T., Wu J. C. S., Chiou C.: *Catal. Commun.* **2008**, *9*, 2073.
4. Wu J. C. S., Lin H., Lai C.: *Appl. Catal., A* **2005**, *296*, 194.
5. Zhang Q., Han W., Hong Y., Yu J. G.: *Catal. Today* **2009**, *148*, 335.
6. Chen S. Z., Zhong S. H.: *Acta Phys.-Chim. Sinica* **2002**, *18*, 1099.
7. Xu A., Gao Y., Liu H.: *J. Catal.* **2002**, *207*, 151.
8. Dey G. R.: *J. Nat. Gas Chem.* **2007**, *16*, 217.
9. Kitano M., Matsuoka M., Ueshima M., Anpo M.: *Appl. Catal., A* **2007**, *325*, 1.
10. Tseng I., Wu J. C. S., Chou H.: *J. Catal.* **2004**, *221*, 432.
11. Xu Y., Liang D., Liu M., Liu D.: *Mater. Res. Bull.* **2008**, *43*, 3474.
12. Yu T., Tan X., Zhao L., Yin Y. X., Chen P., Wei J.: *Chem. Eng. J.* **2010**, *157*, 86.
13. Nguyen T., Wu J. C. S.: *Appl. Catal., A* **2008**, *335*, 112.
14. Ohya S., Kaneco S., Katsumata H., Suzuki T., Ohta K.: *Catal. Today* **2009**, *148*, 329.
15. Slamet, Nasution H. W., Purnama E., Kosela S., Gunlazuardi J.: *Catal. Commun.* **2005**, *6*, 313.
16. Adachi K., Ohta K., Mizuno T.: *Sol. Energy* **1994**, *53*, 187.
17. Yamashita H., Nishiguchi H., Kamada N., Anpo M.: *Res. Chem. Intermed.* **1994**, *20*, 815.
18. Spurr R. A., Myers H.: *Anal. Chem.* **1957**, *29*, 760.
19. Cui Y., Feng Y., Liu Z.: *Electrochim. Acta* **2009**, *54*, 4903.
20. Mcintyre N. S., Cook M. G.: *Anal. Chem.* **1975**, *47*, 2208.
21. Gaarenstroom S. W., Winograd N.: *J. Chem. Phys.* **1977**, *67*, 3500.
22. Kaneco S., Shimizu Y., Ohta K., Mizuno T.: *J. Photochem. Photobiol., A* **1998**, *115*, 223.
23. Linsebigler A. L., Lu G., Yates J. T.: *Chem. Rev.* **1995**, *95*, 735.
24. Hirano K., Inoue K., Yatsu T.: *J. Photochem. Photobiol., A* **1992**, *64*, 255.
25. Wu S. X., Ma Z., Qin Y. N.: *Acta Phys.-Chim. Sinica* **2003**, *19*, 967.
26. Wu S. X., Yin Y. H., He F.: *Photograp. Sci. Photochem.* **2005**, *23*, 333.